EC Accepts, published online ahead of print on 27 December 2013
Eukaryotic Cell doi:10.1128/EC.00271-13

Solanesyl diphosphate synthase, an enzyme of the ubiquinone synthetic pathway, is required throughout the life cycle of *Trypanosoma brucei*†

De-Hua Lai,[a,b*] Estefanía Poropat,[c] Carlos Pravia,[c] Malena Landoni,[d] Alicia S. Couto,[d] Fernando G. Pérez Rojo,[e] Alicia G. Fuchs,[c,e] Marta Dubin,[f] Igal Elingold,[f] Juan B. Rodríguez,[g] Marcela Ferella,[h] Mónica I. Esteva,[c] Esteban J. Bontempi,[a,c,#] and Julius Lukeš[a,b,#]

Biology Centre, Institute of Parasitology[a], and Faculty of Sciences, University of South Bohemia, České Budějovice (Budweis), Czech Republic[b]; Instituto Nacional de Parasitología "Dr. M. Fatala Chabén", Ministerio de Salud, Buenos Aires, Argentina[c]; CIHIDECAR, Departamento de Química Orgánica, Facultad de Ciencias Exactas y Naturales, Universidad de Buenos Aires, Buenos Aires, Argentina[d]; CAECIHS, Universidad Abierta Interamericana, Buenos Aires, Argentina[e];CEFYBO, UBA-CONICET, Facultad de Medicina, Buenos Aires, Argentina[f]; Departamento de Química Orgánica and UMYMFOR (CONICET-FCEyN), Facultad de Ciencias Exactas y Naturales, Universidad de Buenos Aires, Buenos Aires, Argentina[g]; Department of Genetics & Pathology, Rudbeck Laboratory, Uppsala University, Uppsala, Sweden[h].

#Address correspondence to Esteban Bontempi, ejbon@yahoo.com; or Julius Lukeš, jula@paru.cas.cz.

[*] Present address: Center for Parasitic Organisms, State Key Laboratory of Biocontrol, School of Life Sciences, Sun Yat-Sen University, Guangzhou, P.R. China.

† Supplemental material for this article may be found at http://ec.asm.org/.

Running Head: *T. brucei* Solanesyl Diphosphate Synthase

ABSTRACT

Ubiquinone 9 (UQ9), the expected product of the long-chain solanesyl diphosphate synthase (TbSPPS), has a central role in reoxidation of reducing equivalents in the mitochondrion of *Trypanosoma brucei*. The ablation of TbSPPS gene expression by RNAi increased the generation of reactive oxygen species and reduced cell growth and oxygen consumption. The addition of glycerol to the culture medium exacerbated the phenotype by blocking the endogenous generation and excretion of UQ9. The participation of TbSPPS in UQ synthesis was further confirmed by growth rescue using UQ with 10 isoprenyl subunits (UQ10). Furthermore, the survival of infected mice was prolonged upon the down-regulation of TbSPPS and/or the addition of glycerol to drinking water. TbSPPS is inhibited by 1-[(n-oct-1-ylamino)ethyl] 1,1-bisphosphonic acid, and treatment with this compound was lethal for the cells. The findings that both UQ9 and ATP pools were severely depleted by the drug, and that exogenous UQ10 was able to fully rescue growth of the inhibited parasites, strongly suggest that TbSPPS and UQ synthesis were the main targets of the drug. These two strategies highlight the importance of TbSPPS for *T. brucei*, justifying further efforts to validate it as a new drug target.

Keywords: sleeping sickness, inhibitor, chemotherapy, solanesyl diphosphate synthase, *Trypanosoma brucei*, ubiquinone.

INTRODUCTION

The haemoflagellate parasite *Trypanosoma brucei* is responsible for sleeping sickness, a serious disease affecting humans and other vertebrates in sub-Saharan Africa. The main drugs used for treatment have numerous side effects, some are complicated to administer, and poor efficiency with increasing incidence of drug resistance has been reported (1). Therefore, new drugs targeting essential metabolic pathways are urgently needed.

We are interested in polyprenyl diphosphate synthases, enzymes catalyzing the elongation of isoprenoid chains through the condensation of isopentenyl pyrophosphate (5-carbon unit, C5) with allylic prenyl pyrophosphates (2) to produce chains of variable length. The detection of prenylated proteins showed that short isoprenoid chains, both farnesyl and geranygeranyl, are indeed being attached to proteins in this protist (3, 4). Activities of two key enzymes of this pathway in *T. brucei*, namely farnesyl diphosphate synthase and farnesyl transferase, have been characterized (5, 6, 7). Moreover, promising inhibitors of farnesyl diphosphate synthase with anti-parasitic activities have been tested *in vitro* (8, 9, 10) and *in vivo* (11).

On the other hand, enzymes synthesizing longer isoprenoid chains have so far not been thoroughly studied in trypanosomatids (9, 12). Their product is likely to be incorporated into ubiquinone that has a central role in respiration of *T. brucei*, which has two well-studied metabolically distinct stages in its life cycle. The bloodstream forms (BSF), present in vertebrate blood, respires solely via trypanosome alternative oxidase (TAO), while the procyclic forms (PCF), occurring in the tse-tse fly vector, uses both TAO and cytochrome *c*-containing respiratory chain (for reviews see 13, 14). Although UQs of different lengths have

been found in various parasitic protists (12, 15), so far only UQ9 was detected in the BSF of *T. brucei* via mevalonate, its labeled precursor (16, 17).

Due to the importance of UQ in the parasite's metabolism we decided to study TbSPPS (*T. brucei* solanesyl diphosphate synthase), which is responsible for the synthesis of 9 isoprenyl subunits chains. Alterations in the UQ level may affect oxygen consumption, reoxidation of NADH and the ATP pool. Indirectly, the mitochondrial membrane potential in PCF, which is produced via the respiratory chain as in most other aerobic eukaryotes, could decrease. The situation is different for the mammalian-infective BSF cells, which uniquely generate the same potential through the ATP-consuming reverse action of ATP synthase (18). Since UQ participates in the regeneration of the NADH required for ATP synthesis in the glycosomes, the shortage of reduced cofactor is likely to decrease the ATP level in this compartment, as well as in the cytoplasm and mitochondrion.

Reactive oxygen species (ROS) is mostly generated at a low rate as a byproduct of the respiratory chain, mainly from complexes I and III (19, 20). Having a central position in the respiratory chain, UQ receives in a typical cell electrons from complexes I and II and, if present, from alternative NADH dehydrogenase. While both the presence and activity in the *T. brucei* PCF of complex II and rotenone-insensitive alternative NADH dehydrogenase are undisputed (13, 14, 21, 22), both the composition (23, 24) and activity of complex I seems to be highly unusual (25, 26). Diminishing the cellular concentration of UQ could then favor an increase of the reduced NADH pool with parallel formation of ubisemiquinone, facilitating the deviation of electrons to oxygen with consequent mitochondrial ROS formation. A lower amount of UQ could also affect its function in membranes outside the mitochondrion, where it reduces lipid peroxyl radicals and radical scavengers like α-tocopheryl and, together with the

cytochrome *b5* reductase, whose gene is present in the *T. brucei* genome, even assists in extracellular ascorbate stabilization (27). Hence, the depletion of the UQ pool in *T. brucei* may disrupt the redox equilibrium, increasing ROS through a multifaceted action.

Indeed, the down-regulation of the mitochondrion-confined TbSPPS (28) triggered serious metabolic effects in both life stages of *T. brucei*. These effects were mimicked in the wild type cells by the TbSPPS bisphosphonate inhibitor, 1-[(n-oct-1-ylamino)ethyl] 1,1-bisphosphonic acid (compound 1) (9). *In vivo*, infected mice displayed longer survival when TbSPPS was ablated by RNAi, confirming its importance in the metabolism of the parasite.

MATERIALS AND METHODS

Materials. Compound 1 was prepared as previously described (9). Nickel-nitrilotriacetic acid-agarose was obtained from Qiagen (USA), and paraquat, dihydroethidium and UQ10 were provided by Sigma (USA). UQ10/ß-cyclodextrin (a kind gift from A. Šmidovnik) is a complex of 7.5% UQ10 (Bulk Medicines & Pharma, Germany) and ß- cyclodextrin (Xi'an HongChang Pharma, China). Tetramethylrhodamine ethyl ester (TMRE) was purchased from Molecular Probes (USA), Mitotracker Deep Red and CellTiter-Glo® Reagent were obtained from Invitrogen (USA) and Promega (USA), respectively.

DNA sequencing and bioinformatics. The entire coding sequence of the TbSPPS gene was PCR amplified from genomic DNA (strain 29-13) using primers PreBru1 5'-CCTCGAGATCTATGCACCGTGCTAATATTATAT -3' and PreBru2 5'-CCAAGCTTCACAATTCCCGTGTCAGG -3' that introduced *Bgl*II and *Hind*III restriction

sites, respectively, for convenient cloning into the p2T7-177 RNAi and expression vectors. Besides, primer PreBru1 contains an *Xho*I restriction site, which was used for cloning into the pZJM RNAi vector. All constructs were verified by sequencing. Homology searches were performed using Blast or GeneDB, and sequences were aligned using ClustalX 1.81. The molecular weight and isoelectric point were obtained from the ExPASy Server (cn.expasy.org).

Determination of EC_{50}.

Parasites were adjusted to an initial concentration of 5 x 10^4 BSF or 1 x 10^6 PCF ml^{-1} in 200 µl medium and loaded into sterile 96 well plates. Two-fold serial dilutions of compound 1 (boiled to insure complete dissolution and sterility) were added to duplicate wells. After three days, cells in all wells were counted with a Neubauer hemocytometer. Each assay was repeated three times. The EC_{50} (effective concentration for half-maximal growth inhibition) was determined using the CompuSyn software (http://www.combosyn.com/index.html) (29).

Plasmid constructs, transfections, cloning, RNAi induction, and cultivation. The full-size TbSPPS gene (1080 bp) was cloned into the pZJM (30) and p2T7-177 (31) vectors using the *Xho*I, *Bgl*II and *Hind*III sites included in the primer sequences. *T. brucei* PCF 29-13 and BSF single marker (SM) cell lines, were transfected with the linearized constructs, and selected as described elsewhere (32, 33). The PCF flagellates were cultured at 27ºC in SDM79 medium supplied with 15 µg ml^{-1} neomycin G418 and 50 µg ml^{-1} hygromycin, diluted to 10^6 cells ml^{-1} every other day, while BSF were kept at 37ºC in HMI-11 medium with 2.5 µg ml^{-1} G418 and 5% CO_2, and diluted to 10^5 cells ml^{-1} every other day. Phleomycin-resistant transfectants of both stages (2.5 or 1.3 µg ml^{-1}) were cloned by limiting dilution, and RNAi was induced by

adding 1 µg ml^{-1} tetracycline to the medium. Lister 427 PCF (29-13) and BSF (90-13) cell lines (34) were used for the inhibition experiments. Cell concentration was determined using a Neubauer hemocytometer or the Z2 Coulter Counter (USA).

Northern and western blot analyses. Total RNA was isolated using Trizol (Sigma) and 10 µg of RNA per lane was loaded on a 1% formaldehyde agarose gel, blotted, linked to the membrane, and hybridized with a radiolabelled probe under conditions described elsewhere (35). Total cell lysates were separated on 12% SDS-PAGE gels, transferred to membranes and probed with polyclonal antibodies against RNA binding protein 16 (RBP16) (kindly provided by L. Read) and against TbSPPS at 1:1,000 dilutions (28). Appropriate secondary antibodies (1:2,000) (Sevapharma, Czech Rep.) coupled to horseradish peroxidase were visualized using the ECL kit according to the manufacturer's protocol (Pierce, USA).

Measurement of respiration rate, $\Delta\Psi_m$ and reactive oxygen species. Oxygen consumption of both stages was measured as described elsewhere (35, 36). Changes of ROS or the $\Delta\Psi_m$ were determined using the FACSCalibur or the FACSAria flow cytometers (Becton-Dickinson, USA), after the addition of dihydroethidium, TMRE or Mitotracker Deep Red to the cell suspensions (10^6 cells ml^{-1}) at final concentrations of 15 µM, 250 nM or 500 nM, respectively, with carbonyl cyanide m-chlorophenyl hydrazine (CCCP) at a final concentration of 20 µM used as a control. A total of 10,000 events were acquired in the region previously established as that corresponding to the parasites. Data were analyzed with one-way analysis of variance (ANOVA). Significant differences among means were identified by Tukey and Dunnett post-tests and $p \leq 0.05$ was adopted as the minimum criterion of significance.

Statistical analyses were performed using the GraphPad Software. Alterations in the fluorescence were quantified as the percentage of its variation compared with untreated parasites used as a control. The data shown in the graphs are expressed as means ± standard deviation of at least two independent experiments.

***In vivo* infectivity and glycerol treatment.** Mice had food and fresh water available *ad libitum*. Housing conditions, care, handling and euthanasia method were approved by our Institution's Animal Ethics Committee. To determine infectivity of trypanosomes depleted for TbSPPS, four groups of CD-1 mice (5 animals each) were infected intraperitoneally with 100,000 BSF RNAi cells. In their drinking water the first group received 1 mg ml^{-1} doxycycline (AppiChem, USA) sweetened with 50 mg ml^{-1} of sucrose, starting two days before the infection. The second group received 5% glycerol in the drinking water, while the third group received both glycerol and doxycycline. The control group was supplied with pure drinking water. The survival was recorded at least twice a day.

High-performance liquid chromatography. To calibrate the column, the following molecules were run: UQ8 extracted with hexane from *E. coli*, UQ9 isolated from *T. brucei*, and commercially available UQ10. Treated (1 µM compound 1) and untreated BSF were pelleted and diluted in 1 ml methanol. As an internal standard, a known amount of UQ10 was added. The samples were extracted twice with 1 ml hexane. Both extractions were pooled, dried under nitrogen flow, and dissolved in hexane. Samples were analyzed in a HPLC Waters apparatus using a Supelco C-18 column at 0.7 ml min^{-1} flow. The mobile phase was methanol: hexane, 80:20, v/v, isocratic, the loop was 5 µl and the detection was at 275 nm. All solvents were

HPLC grade. The amount of UQ9 was quantified from the area under the curve by comparison with the UQ10 standard.

Measurement of ATP content. An equal volume of the CellTiter-Glo® Reagent (Promega, USA) was added to *T. brucei*, and after a 10 min-long incubation, luminescence was read in a Glomax Multidetection System (Promega). The signal was directly related ($r^2 = 0.99$) to the cell number per well, in the range of 30,000 to 500,000 cells. The luminescence produced by serum-supplemented HMI-11 medium alone was two orders of magnitude lower than that produced by the flagellates.

RESULTS

TbSPPS gene. The *T. cruzi* TcSPPS gene used as a query identified a single *T. brucei* gene (Tb09.160.4300) encoding a protein with calculated molecular weight of 39.2 kDa and an isoelectric point of 6.12. The alignment of TbSPPS and TcSPPS revealed in both proteins the presence of seven regions related to catalysis or binding (37, 38) (see Fig. S1). The TbSPPS gene, identical in strains 29-13 and TREU927/4, is highly conserved between *T. brucei* and *T. cruzi*, as there is 66% and 68% identity (83% similarity) at the nucleotide and amino acid levels, respectively (see Fig. S1 in the supplemental material). Additionally, alanine occupy position -5 before the first and second aspartate-rich motif (Fig. S1), allowing elongation of the isoprenoid chain over C15 (39).

Inhibition of TbSPPS expression by RNAi. To assess the importance of the protein for parasite's metabolism, PCF and BSF cells were transfected with the pZJM and p2T7-177 RNAi vectors, each bearing a full-length TbSPPS gene, respectively. First, total RNA was isolated from the non-induced and RNAi-induced PCF clonal cell line and analyzed by Northern blotting. In the parental 29-13 cell, TbSPPS is abundantly transcribed (band of ~1.9 kb-long. Fig. 1A; also see Fig. S1 in the supplemental material), but probably due to small leakage of the T7 promoter, less TbSPPS mRNA is present in the non-induced cells (clone 4). This effect is likely reflected also by the slight growth inhibition of the non-induced cells, as compared to the 29-13 parentals (Fig. 2A). Upon induction of RNAi with tetracycline, the TbSPPS mRNA was undetectable after two days, with a concurrent massive appearance of double-stranded RNA (Fig. 1A), yet a slow growth phenotype of PCF started only from day 7 (Fig. 2A). Based on the growth curve, day 6 post-RNAi induction was selected for all subsequent experiments. At this time point, the levels of the TbSPPS mRNA and corresponding protein became undetectable by Northern and western blot analyses (Fig. 1A), confirming high efficiency of RNAi.

Viability of the BSF cells was also compromised upon RNAi induction. As revealed by western blot analysis, TbSPPS was equally abundant in the parental SM and the non-induced cells (clone 6), while the protein was downregulated already on day 3 post-induction (Fig. 1B). As judged by the amount of the protein, there seems to be no leakage. Although the disappearance of TbSPPS upon RNAi induction was not complete, growth inhibition started already from day 2 (Fig. 2B).

Diminished O_2 consumption. As shown in Fig. 3, respiration of the non-induced PCF cells represents about 90% of that of the parental cell line and remained the same during the first few

days after RNAi induction. However, on day 6, the oxygen consumption rate of the RNAi-induced cells dropped to approximately 60%, in correlation with the appearance of the growth phenotype. The diminished O_2 consumption then lasted till day 10 post-induction, when the measurement was finished (Fig. 3). Cyanide (KCN) and salicylhydroxamic acid (SHAM), inhibitors of the cytochrome *c* oxidase (= complex IV) and TAO, respectively, were used to discriminate between the oxygen consumption of each pathway. Upon RNAi induction, no switch from one pathway to the other was observed, indicating that the decreased oxygen consumption rate was caused by both of them (Fig. 3A; also see Fig. S3A-E). On the other hand, the oxygen consumption of BSF that rely solely on TAO, dropped on day 3 post-RNAi induction to 50% as compared to the parental and non-induced parasites (Fig. 3B and Fig. S3F).

Inhibition of BSF RNAi cells by glycerol or compound 1. Under hypoxic or anaerobic conditions, glycerol-3-phosphate and ADP accumulate within the glycosomes, causing the glycerol kinase to operate in reverse and excrete glycerol (40). Under these conditions, exogenous glycerol added to the medium became a toxic metabolite, as it may diffuse into the cells, inhibiting the glycerol kinase activity and preventing NAD^+ regeneration (41). Since the ablation of TbSPPS by RNAi will decrease the function of the glycerol-3-phosphate shuttle, the addition of glycerol should further enhance the ensuing phenotype. Indeed, while the addition of 4 mM glycerol to the HMI-11 medium within 5 days had just a mild inhibitory effect on the parental BSF cells (3.4x slower growth) and the non-induced TbSPPS BSF cells (5.2x slower growth), on their RNAi-induced counterparts the effect was dramatic (48.7x slower growth) (Fig. 4A).

Next, we examined the effect of 1-[(n-oct-1-ylamino)ethyl] 1,1-bisphosphonic acid, termed here compound 1, which is a TbSPPS bisphosphonate inhibitor (Fig. 4B). After the addition of compound 1 (1 μM), BSF cells (SM)'s oxygen consumption dropped within 24 hrs to 30%, as compared to the non-treated parasites (Fig. 3B; also see Fig. S3F), but without severe growth defect (Fig. 4C). When trying on the RNAi-induced cells, a strong growth inhibition occurred in the presence of the same concentration (lower than the $EC_{50,}$ see below). Cells grew normally for the first two days, but died suddenly on day 3 (Fig. 4C). It should be noted that this effect could not be mimicked even by treating the parental BSF with the simultaneous addition of compound 1 and 4 mM glycerol (22.9x growth inhibition), suggesting that a minimal amount of the active enzyme is sufficient to support the growth.

Measurement of ROS and mitochondrial membrane potential, and paraquat treatment. Mitotracker and TMRE are fluorophores sensitive to the mitochondrial membrane potential ($\Delta\Psi_m$) that stain functional mitochondria. Flagellates from both stages depleted for TbSPPS did not show any significant increase of the potential as compared to the parental cells. To follow another possible outcome of the disruption of the respiratory system, we have detected the generation of ROS using dihydroethidium. Indeed, in the PCF cells ROS increased continuously, reaching a maximum between days 6 and 8 (Fig. 5A). RNAi-induced BSF did not show any change in fluorescence upon addition of dihydroethidium, suggesting no changes in ROS generation (data not shown). The different phenotypes between two cell forms suggested that the dramatic increase of ROS in the PCF flagellates was likely generated by the disruption of the respiratory chain, which is active only in this life cycle stage.

To corroborate this result, paraquat, a reagent catalyzing ROS formation (42), was added at concentrations ranging from 0.5 to 2 µM to the non-induced and RNAi-induced PCF on day 5. Twenty four hours later an increment in ROS production that lasted several days was detected by flow cytometry (data not shown). The effect was paralleled by a significant growth inhibition on day 8 observed in the paraquat-treated RNAi-induced cells as compared to their equally treated non-induced counterparts (Fig. 5B). Thus, the ROS boost in knock-down cells was responsible for their increased sensitivity to paraquat.

Rescue of RNAi by exogenous UQ and *in vivo* infections. Addition of UQ, the downstream product of SPPS, to the medium should alleviate the effect of RNAi-mediated depletion of TbSPPS. To increase its hydrophilicity and bioavailability, UQ is usually provided bound to other compounds. We used a complex of UQ10 with ß-cyclodextrin, a molecule widely used by the pharmaceutical industry for encapsulation (43). Cells ablated for TbSPPS were subjected to three different concentrations (1, 10 and 90 µM) of the above-mentioned compound added to the cultivation medium. The growth of parental cells (SM) was considered as 100%. In non-induced BSF cells, there was no effect of any of these concentrations on the growth (89-95% growth). While RNAi-induced parasites (56% growth) were marginally affected upon the addition of 1 µM of UQ/ß-cyclodextrin (65% growth), a significant rescue (79% and 85% growth) was observed in the presence of 10 µM and 90 µM of these compounds, respectively (see Fig. S2). After the addition of UQ10, the oxygen consumption returned to normal as compared to the parental and non-induced parasites (Fig. 3B; also see Fig. S3F).

Next, we tested infection of animals with the transfected parasites. In humans, ingested glycerol can raise the serum concentration to 20 mM, from the normal 0.05 mM level (44). In

297 *T. brucei*-infected animals, glycerol added to the drinking water improved the protective effect
298 of ascofuranone (45). Four groups of mice, each composed of five animals, were infected with
299 the same dose of 100,000 BSF RNAi transfectants treated with different substances, with their
300 survival rate being recorded. Two replications of this experimental setup were done with
301 similar results, and one of them is shown (Fig. 6). While four days was the average survival of
302 animals in the control group supplied with plain drinking water, the survival rate increased
303 significantly to 7 and 7.6 days for mice drinking water containing glycerol or doxycycline,
304 respectively. Moreover, the longest average survival of 11.2 days was recorded for animals
305 supplied with drinking water containing both substances (Fig. 6).
306
307 **Metabolic effects of compound 1 on *T. brucei*.** Compound 1 was shown to be a potent
308 inhibitor of the *T. cruzi* SPPS, with an EC_{50} of 250 nM (9). Due to similarities in the active site
309 and in the enzymatic mechanism of type E-polyprenyl diphosphate synthases, we hypothesized
310 that compound 1 could also be active against the TbSPPS protein. Indeed, it affected also the
311 growth of both *T. brucei* life forms, with EC_{50} of 2 µM for BSF as compared to EC_{50} of 50 µM
312 for PCF.
313 Since TbSPPS was predicted to synthesize the isoprenoid chain of UQ9, the expected
314 effect of compound 1 treatment should be the depletion of the UQ pool. The BSF parasites were
315 treated with the inhibitor at a concentration close to its EC_{50}, and UQ was extracted and
316 separated by HPLC. As anticipated, a significant reduction of the UQ9 pool (90 %) was
317 observed under these conditions (Fig. 7A), as compared to extraction standard (UQ10).
318 UQ mediates the transfer of electrons that, through the respiratory chain and/or the
319 glycerol 3- phosphate:dihydroxyacetone-phosphate shuttle, are passed to oxygen as the final

acceptor. We have shown the oxygen consumption of cells incubated with compound 1 in Fig. 3. When increased concentrations of compound 1 were used, the respiration could even drop down to 13% in BSF and 16% in PCF, as compared to the non-treated cells. As with targeting TbSPPS by RNAi, there was no switch from KCN-sensitive to SHAM-sensitive respiration in the inhibited parasites (see Fig. S3). Trypanosomes reoxidize their NADH pool through respiration. After inhibition by compound 1, the reduced rate of reoxidation could be insufficient to provide enough ATP by glycolysis. We have measured the ATP pool in BSF using a luminescent assay. The results were expressed in luminescent arbitrary units (lau) per 5 x 10^4 BSF cells. In comparison with untreated cells (1.4 x 10^5 ± 28000 lau), treatment with 2 µM of compound 1 lowered the signal to 6.75 x 10^4 lau, which represents a 51 % decrease.

We then tested the $\Delta\Psi_m$ variation. Low concentrations of compound 1 produced a mild increase of the potential, while concentrations exceeding the respective EC_{50} caused its slight decrease in both life stages, being significant (10-20%) only in PCF (Fig. 7B). Dissipation of 80% of the potential by the addition of the uncoupler CCCP served as a negative control. As respiratory chain is a major source of ROS (46), any of its alterations are expected to generate more ROS. When compared with the single peak of the untreated cells, PCF incubated with compound 1 formed a population with 25-35% higher amount of ROS, and an additional population with less fluorescent particles (Fig. 7C). The BSF cells, which lack a functional respiratory chain, either depleted for TbSPPS or treated with compound 1 still generate a normal amount of ROS. However, similarly to PCF, higher concentrations of the inhibitor generated a second peak with a lower ROS concentration, likely representing dead or dying cells.

342 Next, we tested whether UQ10 could rescue the growth inhibition of the 90-13 BSF cell line
343 caused by treatment with compound 1. The inhibitor was used at a concentration of 10 µM,
344 which is lethal for BSF within three days. To eliminate the possibility of the inhibitor getting
345 trapped by ß-cyclodextrin, we added commercial UQ10 alone to the medium. In spite of the
346 limited aqueous solubility of the bisphosphonate, the lethal phenotype was fully superseded in
347 the presence of 20 µM UQ10, as the BSF cells grew at a normal rate (Fig. 7D).
348
349 **DISCUSSION**
350
351 In an effort to find novel chemotherapeutic targets against pathogenic trypanosomatids, we
352 decided to study the long chain polyprenyl diphosphate synthases. Earlier, SPPS of *T. cruzi* was
353 characterized (12), with some bisphosphonate inhibitors tested against the recombinant enzyme
354 (9). In order to further validate these enzymes as putative targets, we performed functional
355 analysis of the corresponding protein in *T. brucei* using RNAi and inhibition by compound 1.
356 This compound was shown to inhibit SPPS and the farnesyl diphosphate synthase of *T. cruzi*
357 (9) and was thus an obvious candidate. The identification of TbSPPS was straightforward due
358 to a high sequence similarity with its *T. cruzi* homologue. The protein was detected in the PCF
359 and BSF cells and the down-regulation by RNAi or the inhibition of TbSPPS affected the
360 growth of both of them.
361 In most cells, UQ is involved in respiration, which is linked to other activities. Defficient
362 respiration would be reflected in diminished oxygen consumption, which was indeed observed
363 in PCF and BSF after RNAi-induction or inhibition with compound 1. Insufficient
364 mitochondrial (and glycosomal) NADH reoxidation would be reflected in lowered total ATP

and altered generation of $\Delta\Psi_m$. The effect of the addition of glycerol to the RNAi-induced BSF highlighted a survival mechanism of cells experiencing an imbalance in the NADH/NAD^+ ratio in glycosomes. In fact, the failure to efficiently reoxidate NADH through the glycerol-3-phosphate:dihydroxyacetone-phosphate shuttle bolstered the production of glycerol by the action of the glycerol-3-phosphate dehydrogenase and the glycerol kinase. Hence, hindering this outlet by the exogenous glycerol seriously affected the cell growth.

Nitrogen-containing bisphosphonates were earlier found to be effective *in vitro* and *in vivo* against *T. cruzi* without toxicity to the host cells (47). From the experiment with compound 1 on RNAi-induced *T. brucei* it can be concluded that TbSPPS is inhibited in the same fashion as TcSPPS, a reflection of the high similarity between their respective active sites. In fact, compound 1 was more efficient than RNAi in abolishing the enzymatic activity of TbSPPS, leading to a lethal phenotype. Regarding the redox balance, a massive build-up of ROS was detected in PCF following RNAi induction, and a similar but lesser effect was seen after the treatment with compound 1. An incremented production of ROS by the respiratory chain could be controlled by mechanisms involving iron-superoxide dismutases, which transform superoxide radicals into oxygen and hydrogen peroxide. As there are four isoforms of these enzymes distributed in glycosomes, cytosol and mitochondria (48, 49), it would be of interest to address whether they are overexpressed in the TbSPPS knock-downs. In conclusion, both in the RNAi knock-down parasites, as well as in those treated with compound 1, neither the generation and maintenance of $\Delta\Psi_m$ nor ROS were the main cause of the phenotype triggered by tampering with TbSPPS.

Without active synthesis of the isoprenyl chain, the UQ pool, estimated to be 0.1 nmol UQ in 10^9 BSF cells (17), should diminish according to its half-life which, however, remains

undetermined in *T. brucei*. The UQ half-life varies in different organisms, ranging in rat tissues between 49 and 125 hrs (50), while in human blood it is about 34 hrs (51). The HPLC results of BSF inhibited for three days confirmed a huge exhaustion of the pool, suggesting that the half-life of *T. brucei* UQ is comparable to that in other organisms. The HPLC experiment also provided additional data about the UQ9 content of *T. brucei* cells. The average value obtained was 1.825 ng/ 10^6 cells, equivalent to 2.3 nmoles/ 10^9 cells. This represents 1.3 million molecules per cell, a value higher than the reported one (17) but still lower than that described from other cells. For example, hepatocytes, cells with a 50 times larger volume, contain 246 million molecules per cell (52).

Aminobisphosphonates caused ATP decrease in a tapeworm model (53), but the molecular mechanism has not been described. In *T. brucei* ATP generation is probably not affected directly by the decrease of TbSPPS. The PCF cells obtain the bulk of ATP by substrate level phosphorylation (54, 55) or via oxidative phosphorylation (35). Through the depletion of NAD^+, however, the interference may indirectly affect these ATP-producing processes. The same is likely to happen in BSF, which metabolize glucose in glycosomes (56) but depend on the NADH reoxidation in mitochondria through the UQ-dependent glycerol-3-phosphate shuttle. Thus, the significant decrease of ATP plausibly caused the growth phenotype and, at longer times or higher concentrations of compound 1, the lethal outcome.

Another factor to be considered is the acquisition of UQ from the serum that may replenish the dwindling intracellular pool, following the RNAi-mediated ablation of TbSPPS or its inhibition via a drug. In several organisms including humans, the UQ deficiency increases the uptake and transport of the exogenous UQ to mitochondria (57, 58). In the serum, UQ is normally transported by lipid particles, such as (very) low as well as high density lipoproteins, which can

411 be uptaken by specific cell receptors, some of which have already been described in *T. brucei*
412 (59 - 61). It was also demonstrated that the parasite's growth is affected in the lipoprotein-free
413 serum or in the presence of anti-receptor antibodies (59, 62).

414 Alone or in a complex with ß-cyclodextrin, UQ10 was apparently taken up by
415 trypanosomes, since the exogenous UQ rescued their growth, which was affected by either
416 RNAi-mediated down-regulation or specific inhibition of TbSPPS. The complementation effect
417 by the exogenous UQ on inhibited parasites clearly pinpoints UQ biosynthesis rather than
418 protein farnesylation as the main target of compound 1. While highlighting the importance of
419 UQ for the BSF cells, the rescue experiments are also in accordance with an earlier report, in
420 which synvinolin (simvastatin) reduced cell growth through the inhibition of the first enzyme of
421 the mevalonate pathway, the 3-hydroxy-3-methylglutaryl coenzyme A reductase (62). This
422 enzyme is responsible for the synthesis of sterols and isoprenoids. The addition of exogenous
423 mevalonate or low density lipoprotein particles, which transport some of the final products of
424 the pathway, almost completely reverted the phenotype. Interestingly, the growth was reverted
425 less efficiently by exogenous cholesterol alone, indicating that another essential products
426 present in the low density lipoprotein particles such as UQ, were depleted by the synvinolin
427 inhibition (62).

428 The experiment in which transfected parasites were RNAi-induced *in vivo* showed that
429 interfering with the synthesis of TbSPPS doubled the life span of the infected mice, confirming
430 the *in vitro* results. Furthermore, as anticipated, the excess of glycerol further substantially
431 prolonged survival of the infected animals. The experiments reported here show that TbSPPS is
432 the main target of compound 1, and also that blocking the biosynthesis of UQ has important
433 metabolic consequences for both *T. brucei* life stages.

434

ACKNOWLEDGEMENTS

We wish to thank Andrej Šmidovnik (National Institute of Chemistry, Ljubljana, Slovenia) for the provision of UQ10/ß-cyclodextrin complex, Claudia Nose (Instituto Nacional de Parasitología, Buenos Aires, Argentina) for art work, Philippe Bastin (Institut Pasteur, Paris, France) for comments on the manuscript and Marcelo Argüelles (Universidad Nacional de Quilmes, Argentina) for help with the flow cytometry experiments. Laurie K. Read (State University of New York, Buffalo, USA) kindly provided antibodies. This work was supported by the FOCANLIS2010, the FOCANLIS2013 and the Instituto Nacional de Parasitología "Dr. Mario Fatala Chabén", A.N.L.I.S. "Dr. Carlos G. Malbrán" to E.J.B., the Grant Agency of the Czech Republic P305/11/2179, project BIOGLOBE CZ.1.07/2.3.00/30.0032, AMVIS LH12104, and the Praemium Academiae award to J.L., who is also a Fellow of the Canadian Institute for Advanced Research.

REFERENCES

1. **Legros D, Ollivier G, Gastellu-Etchegorry M, Paquet C, Burri C, Jannin J, Büscher P.** 2002. Treatment of human African trypanosomiasis--present situation and needs for research and development. Lancet Infect. Dis. **2:**437–440.
2. **Ohnuma S, Hirooka K, Tsuruoka N, Yano M, Ohto C, Nakane H, Nishino T.** 1998. A pathway where polyprenyl diphosphate elongates in prenyltransferase. Insight into a

457 common mechanism of chain length determination of prenyltransferases. J. Biol. Chem.
458 **273:**26705–26713.
459 3. **Yokoyama K, Lin Y, Stuart KD, Gelb MH.** 1997. Prenylation of proteins in *Trypanosoma*
460 *brucei*. Mol. Biochem. Parasitol. **87:**61–69.
461 4. **Field H, Blench I, Croft S, Field MC.** 1996. Characterisation of protein isoprenylation in
462 procyclic form *Trypanosoma brucei*. Mol. Biochem. Parasitol. **82:**67–80.
463 5. **Montalvetti A, Fernandez A, Sanders JM, Ghosh S, Van Brussel E, Oldfield E,**
464 **Docampo R.** 2003. Farnesyl pyrophosphate synthase is an essential enzyme in
465 *Trypanosoma brucei*. *In vitro* RNA interference and *in vivo* inhibition studies. J. Biol.
466 Chem. **278:**17075–17083.
467 6. **Yokoyama K, Trobridge P, Buckner FS, Van Voorhis WC, Stuart KD, Gelb MH.** 1998.
468 Protein farnesyltransferase from *Trypanosoma brucei*: A heterodimer of 61- and 65-kDa
469 subunits as a new target for antiparasite therapeutics. J. Biol. Chem. **273:**26497–26505.
470 7. **Buckner FS, Yokoyama K, Nguyen L, Grewal A, Erdjument-Bromage H, Tempst P,**
471 **Strickland CL, Xiao L, Van Voorhis WC, Gelb MH.** 2000. Cloning, heterologous
472 expression, and distinct substrate specificity of protein farnesyltransferase from
473 *Trypanosoma brucei*. J. Biol. Chem. **275:**21870–21876.
474 8. **Garzoni LR, Caldera A, Meirelles M de N, de Castro SL, Docampo R, Meints GA,**
475 **Oldfield E, Urbina JA.** 2004. Selective *in vitro* effects of the farnesyl pyrophosphate
476 synthase inhibitor risedronate on *Trypanosoma cruzi*. Int. J. Antimicrob. Agents **23:**273–
477 285.
478 9. **Szajnman SH, García Liñares GE, Li ZH, Jiang C, Galizzi M, Bontempi EJ, Ferella M,**
479 **Moreno SN, Docampo R, Rodriguez JB.** 2008. Synthesis and biological evaluation of 2-

480 alkylaminoethyl-1,1-bisphosphonic acids against *Trypanosoma cruzi* and *Toxoplasma*
481 *gondii* targeting farnesyl diphosphate synthase. Bioorg. Med. Chem. **16:**3283–3290.
482 10. **Demoro B, Caruso F, Rossi M, Benítez D, Gonzalez M, Cerecetto H, Parajón-Costa B,**
483 **Castiglioni J, Galizzi M, Docampo R, Otero L, Gambino D.** 2010. Risedronate metal
484 complexes potentially active against Chagas disease. Inorg. Biochem. **104:**1252–1258.
485 11. **Garzoni LR, Waghabi MC, Baptista MM, de Castro SL, Meirelles M de N, Britto CC,**
486 **Docampo R, Oldfield E, Urbina JA.** 2004. Antiparasitic activity of risedronate in a murine
487 model of acute Chagas' disease. Int. J. Antimicrob. Agents **23:**286–290.
488 12. **Ferella M, Montalvetti A, Rohloff P, Miranda K, Fang J, Reina S, Kawamukai M, Búa**
489 **J, Nilsson D, Pravia C, Katzin A, Cassera MB, Aslund L, Andersson B, Docampo R,**
490 **Bontempi EJ.** 2006. A solanesyl-diphosphate synthase localizes in glycosomes of
491 *Trypanosoma cruzi*. J. Biol. Chem. **281:**39339–39348.
492 13. **Besteiro S, Barrett MP, Rivière L, Bringaud F.** 2005. Energy generation in insect stages
493 of *Trypanosoma brucei*: metabolism in flux. Trends Parasitol. **21:**185–191.
494 14. **Tielens AGM, van Hellemond JJ.** 2009. Surprising variety in energy metabolism within
495 Trypanosomatidae. Trends Parasitol. **25:**482–490.
496 15. **Ellis JE, Setchell KDR, Kaneshiro ES.** 1994. Detection of ubiquinone in parasitic and
497 free-living protozoa, including species devoid of mitochondria. Mol. Biochem. Parasitol.
498 **65:**213–224.
499 16. **Clarkson AB, Bienen EJ, Pollakis G, Grady RW.** 1989. Respiration of bloodstream
500 forms of the parasite *Trypanosoma brucei brucei* is dependent on a plant-like alternative
501 oxidase. J. Biol. Chem. **264:**17770–17776.

17. **Löw P, Dallner G, Mayor S, Cohen S, Chait BT, Menon AK.** 1991. The mevalonate pathway in the bloodstream form of *Trypanosoma brucei*. Identification of dolichols containing 11 and 12 isoprene residues. J. Biol. Chem. **266:**19250–19257.

18. **Schnaufer A, Clark-Walker JD, Steinberg AG, Stuart K.** 2005. The F1-ATP synthase complex in bloodstream stage trypanosomes has an unusual and essential function. EMBO J. **24:**4029–4040.

19. **Sugioka K, Nakano M, Totsune-Nakano H, Minakami H, Tero-Kubota S, Ikegami Y.** 1988. Mechanism of O_2- generation in reduction and oxidation cycle of ubiquinones in a model of mitochondrial electron transport systems. Biochim. Biophys. Acta **936:**377–385.

20. **Turrens JF, Boveris A.** 1980. Generation of superoxide anion by the NADH dehydrogenase of bovine heart mitochondria. Biochem. J. **191:**421–427.

21. **Morales J, Mogi T, Mineki S, Takashima E, Mineki R, Hirawake H, Sakamoto K, Omura S, Kita K.** 2009. Novel mitochondrial complex II isolated from *Trypanosoma cruzi* is composed of 12 peptides including a heterodimeric Ip subunit. J. Biol. Chem. **284:**7255–7263.

22. **Fang J, Beattie DS.** 2002. Rotenone-insensitive NADH dehydrogenase is a potential source of superoxide in procyclic *Trypanosoma brucei* mitochondria. Mol. Biochem. Parasitol. **123:**135–142.

23. **Panigrahi AK, Zíková A, Dalley RA, Acestor N, Ogata Y, Anupama A, Myler PJ, Stuart KD.** 2008. Mitochondrial complexes in *Trypanosoma brucei*: a novel complex and a unique oxidoreductase complex. Mol. Cell Proteomics **7:**534–545.

24. **Opperdoes FR, Michels PA.** 2008. Complex I of Trypanosomatidae: does it exist? Trends Parasitol. **24:**310–317.

525 25. **Verner Z, Čermáková P, Škodová I, Kriegová E, Horváth A, Lukeš J.** 2011. Complex I
526 (NADH:ubiquinone oxidoreductase) is active in but non-essential for procyclic
527 *Trypanosoma brucei*. Mol. Biochem. Parasitol. **175:**196–200.
528 26. **Surve S, Heestand M, Panicucci B, Schnaufer A, Parsons M.** 2012. Enigmatic presence
529 of mitochondrial complex I in *Trypanosoma brucei* bloodstream forms. Eukaryot. Cell
530 **11:**183–193.
531 27. **Santos-Ocaña C, Córdoba F, Crane FL, Clarke C F, Navas P.** 1998. Coenzyme Q6 and
532 iron reduction are responsible for the extracellular ascorbate stabilization at the plasma
533 membrane of *Saccharomyces cerevisiae*. J. Biol. Chem. **273:**8099–8105.
534 28. **Lai D-H, Bontempi EJ, Lukeš J.** 2012. *Trypanosoma brucei* solanesyl-diphosphate
535 synthase localizes to the mitochondrion. Mol. Biochem. Parasitol. **183:**189–192.
536 29. **Chou TC.** 2006. Theoretical basis, experimental design, and computerized simulation of
537 synergism and antagonism in drug combination studies. Pharmacol. Rev. **58:**621–681.
538 30. **Wang Z, Morris JC, Drew ME, Englund PT.** 2000. Inhibition of *Trypanosoma brucei*
539 gene expression by RNA interference using an integratable vector with opposing T7
540 promoters. J. Biol. Chem. **275:**40174–40179.
541 31. **Wickstead B, Ersfeld K, Gull K.** 2002. Targeting of a tetracycline-inducible expression
542 system to the transcriptionally silent minichromosomes of *Trypanosoma brucei*. Mol.
543 Biochem. Parasitol. **125:**211–216.
544 32. **Vondrušková E, van den Burg J, Zíková A, Ernst NL, Stuart K, Benne R, Lukeš J.**
545 2005. RNA interference analyses suggest a transcript-specific regulatory role for
546 mitochondrial RNA-binding proteins MRP1 and MRP2 in RNA editing and other RNA
547 processing in *Trypanosoma brucei*. J. Biol. Chem. **280:**2429–2438.

548 33. **Hashimi H, Čičová Z, Novotná L, Wen Y-Z, Lukeš J.** 2009. Kinetoplastid guide RNA
549 biogenesis is dependent on subunits of the mitochondrial RNA binding complex 1 and
550 mitochondrial RNA polymerase. RNA **15:**588–599.
551 34. **Wirtz E, Leal S, Ochatt C, Cross GA.** 1999. A tightly regulated inducible expression
552 system for conditional gene knock-outs and dominant-negative genetics in *Trypanosoma*
553 *brucei*. Mol. Biochem. Parasitol. **99:**89–101.
554 35. **Horváth A, Horáková E, Dunajčíková P, Verner Z, Pravdová E, Šlapetová I,**
555 **Cuninková L, Lukeš J.** 2005. Downregulation of the nuclear-encoded subunits of the
556 complexes III and IV disrupts their respective complexes but not complex I in procyclic
557 *Trypanosoma brucei*. Mol. Microbiol. **58:**116–130.
558 36. **Lai D-H, Hashimi H, Lun ZR, Ayala FJ, Lukeš J.** 2008. Adaptations of *Trypanosoma*
559 *brucei* to gradual loss of kinetoplast DNA: *Trypanosoma equiperdum* and *Trypanosoma*
560 *evansi* are petite mutants of *T. brucei*. Proc. Natl. Acad. Sci. USA **105:**1999–2004.
561 37. **Koyama T.** 1999. Molecular analysis of prenyl chain elongating enzymes. Biosci.
562 Biotechnol. Biochem. **63:**1671–1676.
563 38. **Chen A, Kroon PA, Poulter D.** 1994. Isoprenyl diphosphate synthases: protein sequence
564 comparisons, a phylogenetic tree, and predictions of secondary structure. Prot. Sci. **3:**600–
565 607.
566 39. **Liang P-H, Ko T-P, Wang AH.** 2002. Structure, mechanism and function of
567 prenyltransferases. Eur. J. Biochem. **269:**3339–3354.
568 40. **Krakow JL, Wang CC.** 1990. Purification and characterization of glycerol kinase from
569 *Trypanosoma brucei*. Mol. Biochem. Parasitol. **43:**17-25.

41. **Hammond DJ, Bowman IB.** 1980. Studies on glycerol kinase and its role in ATP synthesis in *Trypanosoma brucei*. Mol. Biochem. Parasitol. **2:**77-91.

42. **Bus JS Gibson JE.** 1984. Paraquat: model for oxidant-initiated toxicity. Environ. Health Perspect. **55:**37–46.

43. **Loftsson T, Duchêne D.** 2006. Cyclodextrins and their pharmaceutical applications. Int. J. Pharm. **329:**1–11.

44. **Robergs RA, Griffin SE**. 1998. Glycerol. Biochemistry, pharmacokinetics and clinical and practical applications. Sports Med. **26:**145-167.

45. **Yabu Y, Minagawa N, Kita K, Nagai K, Honma M, Sakajo S, Koide T, Ohta N, Yoshimoto A.** 1998. Oral and intraperitoneal treatment of *Trypanosoma brucei brucei* with a combination of ascofuranone and glycerol in mice. Parasitol. Internat. **47:**131-137.

46. **Boveris A, Oshino N, Chance B.** 1972. The cellular production of hydrogen peroxide. Biochem. J. **128:**617–630.

47. **Urbina JA, Moreno B, Vierkotter S, Oldfield E, Payares G, Sanoja C, Bailey BN, Yan W, Scott DA, Moreno SN, Docampo R.** 1999. *Trypanosoma cruzi* contains major pyrophosphate stores, and its growth *in vitro* and *in vivo* is blocked by pyrophosphate analogs. J. Biol. Chem. **274:**33609–33615.

48. **Dufernez F, Yernaux C, Gerbod D, Noël C, Chauvenet M, Wintjens R, Edgcomb VP, Capron M, Opperdoes FR, Viscogliosi E.** 2006. The presence of four iron-containing superoxide dismutase isozymes in trypanosomatidae: characterization, subcellular localization, and phylogenetic origin in *Trypanosoma brucei*. Free Rad. Biol. Med. **40:**210–225.

49. **Wilkinson SR, Prathalingam SR, Taylor MC, Ahmed A, Horn D, Kelly JM.** 2006. Functional characterisation of the iron superoxide dismutase gene repertoire in *Trypanosoma brucei*. Free Rad. Biol. Med. **40:**198–209.

50. **Thelin A, Schedin S, Dallner G.** 1992. Half-life of ubiquinone-9 in rat tissues. FEBS Lett. **313:**118–120.

51. **Greenberg S, Frishman WH.** 1990. Co-enzyme Q10: a new drug for cardiovascular disease. J. Clin. Pharmacol. **30:**596–608.

52. **Åstrand I-M, Fries E, Chojnacki T, Dallner G.** 1986. Inhibition of dolichyl phosphate biosynthesis by compactin in cultured rat hepatocytes. Eur. J. Biochem. **155:**447-452.

53. **Fuchs AG, Echeverría CI, Pérez Rojo FG, Prieto González EA, Roldán EJA.** 2013. Proline modulates the effect of bisphosphonate on calcium levels and adenosine: triphosphate production in cell lines derived from bovine *Echinococcus granulosus* protoscoleces. J. Helminthol. **7:**1-9.

54. **Bochud-Allemann N, Schneider A.** 2002. Mitochondrial substrate level phosphorylation is essential for growth of procyclic *Trypanosoma brucei*. J. Biol. Chem. **277:**32849–32854.

55. **Coustou V, Besteiro S, Biran M, Diolez P, Bouchaud V, Voisin P, Michels PA, Canioni P, Baltz T, Bringaud F.** 2003. ATP generation in the *Trypanosoma brucei* procyclic form: cytosolic substrate level is essential, but not oxidative phosphorylation. J. Biol. Chem. **278:**49625–49635.

56. **Opperdoes FR.** 1987. Compartmentation of carbohydrate metabolism in trypanosomes. Annu. Rev. Microbiol. **41:**127–151.

57. **Santos-Ocaña C, Do TQ, Padilla S, Navas P, Clarke CF.** 2002. Uptake of exogenous coenzyme Q and transport to mitochondria is required for bc1 complex stability in yeast coq mutants. J. Biol. Chem. **277:**10973–10981.

58. **Turunen M, Olsson J, Dallner G.** 2004. Metabolism and function of coenzyme Q. Biochim. Biophys. Acta **1660:**171–199.

59. **Coppens I, Baudhuin P, Opperdoes FR, Courtoy PJ.** 1988. Receptors for the host low density lipoproteins on the hemoflagellate *Trypanosoma brucei*: purification and involvement in the growth of the parasite. Proc. Natl. Acad. Sci. USA **85:**6753–6757.

60. **Liu J, Qiao X, Du D, Lee MG.** 2000. Receptor-mediated endocytosis in the procyclic form of *Trypanosoma brucei*. J. Biol. Chem. **275:**12032–12040.

61. **Green HP, Del Pilar Molina Portela M, St. Jean EN, Lugli EB, Raper J.** 2003. Evidence for a *Trypanosoma brucei* lipoprotein scavenger receptor. J. Biol. Chem. **278:**422–427.

62. **Coppens I, Bastin P, Levade T, Courtoy PJ.** 1995. Activity, pharmacological inhibition and biological regulation of 3-hydroxy-3-methylglutaryl coenzyme A reductase in *Trypanosoma brucei*. Mol. Biochem. Parasitol. **69:**29–40.

631 **Figure legends**

632

633 **FIG. 1**. Northern and Western blot analyses of the TbSPPS *T. brucei* RNAi cell lines. (A)
634 Effect of TbSPPS RNAi on mRNA and protein levels in the procyclic stage (clone 4). Total
635 RNA and protein were extracted from parental 29-13 cells (lane 1), non-induced cells (lane 2)
636 and procyclic cells on day 6 after RNAi induction (lane 3). Two upper panels show Northern
637 blot analysis with the full-length TbSPPS gene used as a probe. Ethidium bromide stained
638 rRNAs was used as a loading control. Two lower panels show western blot analysis of the
639 expression of the TbSPPS protein in same cell lines as in the RNA panels. The target protein
640 was detected with specific polyclonal α-TbSPPS antibodies. Antibody against RNA-binding
641 protein 16 (RBP16) was used as a loading control. (B) Effect of TbSPPS RNAi on mRNA and
642 protein levels in the bloodstream stage (clone 6) on day 3 after RNAi induction. Total protein
643 was extracted from parental SM cells (lane 1), non-induced cells (lane 2) and bloodstream cells
644 3 days after RNAi induction (lane 3). TbSPPS and RBP16 were detected as described in (A).

645

646 **FIG. 2**. Effect of TbSPPS RNAi on cell growth of the procyclic (A) and bloodstream (B) cells.
647 Cell densities (cells ml^{-1}) of procyclics and bloodstreams were measured and diluted as
648 explained. The total cell numbers were calculated and plotted on a logarithmic scale on the *y*-
649 axis over 14 days (A) or 6 days (B). Clonal procyclics (A) and bloodstreams (B) grown in the
650 absence or presence of 1 mg ml^{-1} tetracycline, the addition of which induces RNAi, are
651 indicated by dotted lines with empty triangles and continuous lines with black triangles,
652 respectively. The growth of parental procyclics (29-13) and bloodstreams (SM) is shown by a
653 dotted line with empty circles.

654

655 **FIG. 3**. Effect of TbSPPS RNAi on oxygen consumption rate in the procyclic (A) and
656 bloodstream (B) cells. (A) For procyclics, the relative contribution of alternative pathway via
657 trypanosome alternative oxidase (TAO; black columns) and cytochrome-mediated pathway
658 (OXPHOS; white columns) was measured in parental 29-13 cells, non-induced cells (-), and
659 cells 2, 6 and 10 days after RNAi induction. The amount of O_2 consumption inhibited by KCN
660 (0.1 mM) reflected the capacity of the cytochrome-mediated pathway, while the amount
661 inhibited by SHAM (0.03 mM) represented the TAO activity. The non-inhibited residual
662 oxygen consumption was considered as zero. The mean and the S.D. values of three
663 experiments are shown. (B) In the absence of the cytochrome-mediated pathway in the
664 bloodstream cells, all respiration is mediated by TAO. Oxygen consumption was measured in
665 parental SM cells, non-induced cells (-), cells after 1 or 3 days RNAi induction, cells after
666 compound 1 (1 µM for 24 hours) inhibition and RNAi cells supplied with UQ10. Statistic
667 significances to control group were indicated by asterisks (*, $p<0.05$; ***, $p<0.0005$; ****,
668 $p<0.00005$).

669

670 **FIG. 4**. Growth curve of bloodstream transfectant cells in the presence of glycerol or
671 compound 1. (A) The addition of 4 mM glycerol to the medium had an inhibitory effect on the
672 TbSPPS knock-downs after RNAi induction (continuous line with full squares), while only
673 mild effect was observed for the SM parental (continuous line with full circles) and non-
674 induced cells (continuous line with full triangles). The same cell lines were grown in the
675 absence of glycerol as controls (dotted lines). (B) Chemical structure of 1-[(n-oct-1-
676 ylamino)ethyl] 1,1-bisphosphonic acid (compound 1), a potent inhibitor of the enzymatic

activity of TcSPPS. (C) The addition of 1 µM compound 1 to the medium was lethal for the RNAi-induced TbSPPS knock-downs (continuous line with full squares), while just a very small effect was observed for the SM parental (continuous line with full circles) and the non-induced cells (continuous line with full triangles). The same cell lines were grown in the absence of compound 1 as controls (dotted lines). The experiment was repeated three times, a representative curve is shown.

FIG. 5. Generation of reactive oxygen species (A) and paraquat treatment (B) in the TbSPPS procyclic cells. Experiments were performed at least twice with triplicate samples. (A) Parental 29-13 cells (open area with black line), non-induced cells (gray area) and procyclics 6 days after RNAi induction (open area with gray line) were incubated in the presence of 5 mg ml^{-1} dihydroethidium for 30 min. The fluorescence distributions measured by flow cytometry were plotted as frequency histograms. (B) Growth of procyclics, non-induced (open boxes) or cells induced by RNAi for 5 days (gray boxes), incubated for 3 additional days in the presence of 0.2, 0.5, 1 and 2 µM paraquat. The growth of cells in the absence of paraquat, either non-induced or RNAi-induced, was considered as 100%. Statistic significances between two groups were indicated by asterisks (***, $p<0.0005$; ****, $p<0.00005$)

FIG. 6. Survival of mice infected with TbSPPS RNAi transfectant cells was prolonged upon the addition of glycerol and doxycycline. Drinking water available to four groups of mice, each consisting of five individuals, was either pure (gray line), or supplemented with 1 mg ml^{-1} doxycyline sweetened with 50 mg ml^{-1} of sucrose (black line), or 5% glycerol (black dotted

line), or both doxycycline and glycerol (gray dotted line). The survival of mice was followed on a daily basis.

FIG. 7. Metabolic effects of the inhibition by compound 1 on wild type bloodstreams. (A) Measurement of the UQ pool. HPLC representative runs for untreated and treated bloodstreams are shown. The positions of the calibration standards are indicated by arrows. (B) The $\Delta\Psi_m$ displayed by procyclics treated with different concentrations of compound 1. Statistical analysis and a representative experiment are presented. Asterisks indicate significant differences in comparison to the control group (untreated parasites). The arrowhead represents the position of the depolarized membrane control CCCP. (C) ROS level in procyclics treated for 72 hrs with 50 µM compound 1. The data is expressed as means ± standard deviation of at least two independent experiments. (D) Rescue of parental SM bloodstream cells. The addition of 10 µM compound 1 to the medium was lethal within three days (continuous line with full squares). Further addition of 20 µM UQ10 fully rescued cell growth (continuous line with full circles). Non-treated (empty squares) and cells treated only with UQ10 (empty circles) were used as controls.

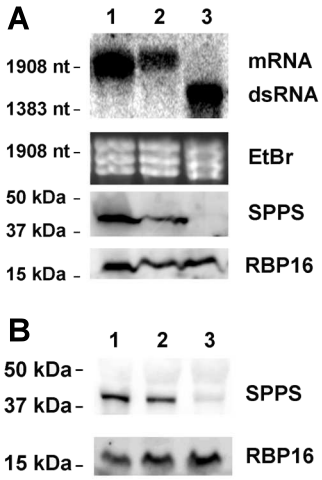

FIG. 1. Northern and Western blot analyses of the TbSPPS T. brucei RNAi cell lines. (A) Effect of TbSPPS RNAi on mRNA and protein levels in the procyclic stage (clone 4). Total RNA and protein were extracted from parental 29-13 cells (lane 1), noninduced RNAi cells (lane 2) and procyclic cells on day 6 after RNAi induction (lane 3). Two upper panels show Northern blot analysis, with the full-length TbSPPS gene used as a probe. Ethidium bromide stained rRNAs was used as a loading control. Two lower panels show Western blot analysis of the expression of the TbSPPS protein in same cell lines as in the RNA panels. The target protein was detected with specific polyclonal TbSPPS antibodies. Antibody against RNA-binding protein 16 (RBP16) was used as a loading control. (B) Effect of TbSPPS RNAi on mRNA and protein levels in the bloodstream stage (clone C6) on day 3 after RNAi induction. Total protein was extracted from parental SM cells (lane 1), non-induced RNAi cells (lane 2) and bloodstream cells 3 days after RNAi induction (lane 3). TbSPPS and RBP16 were detected as described in (A).

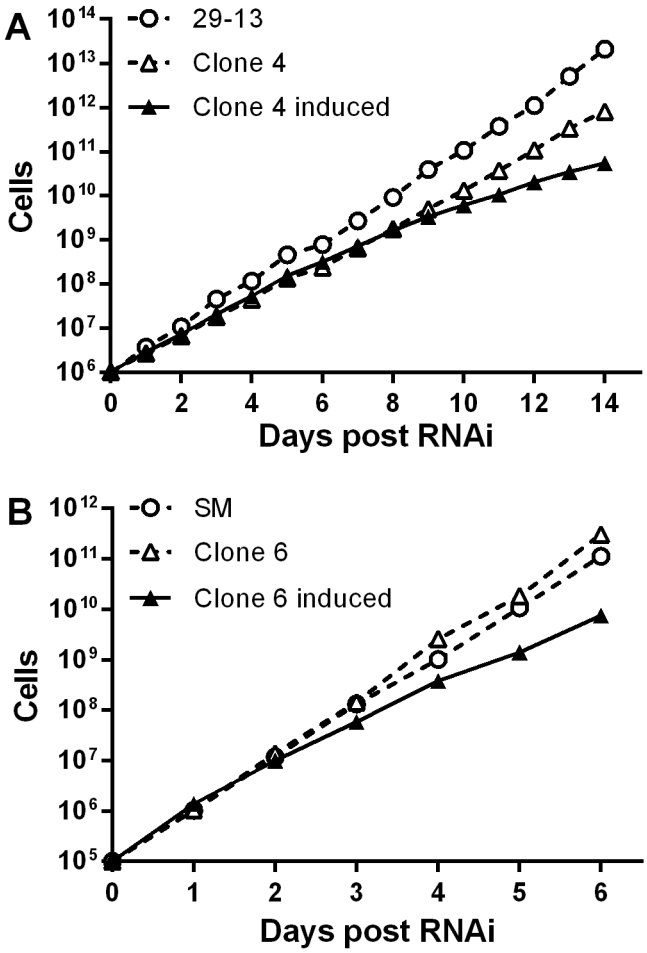

FIG. 2. Effect of TbSPPS RNAi on cell growth of the procyclic (A) and bloodstream (B) cells. Cell densities (cells ml^{-1}) of procyclics and bloodstreams were measured and diluted as explained. The total cell numbers were calculated and plotted on a logarithmic scale on the y-axis over 14 days (A) or 6 days (B). Clonal procyclics (A) and bloodstreams (B) grown in the absence or presence of 1 mg ml^{-1} tetracycline, the addition of which induces RNAi, are indicated by dotted lines with empty triangles and continuous lines with black triangles, respectively. The growth of parental procyclics (29-13) and bloodstreams (SM) is shown by a dotted line with empty circles.

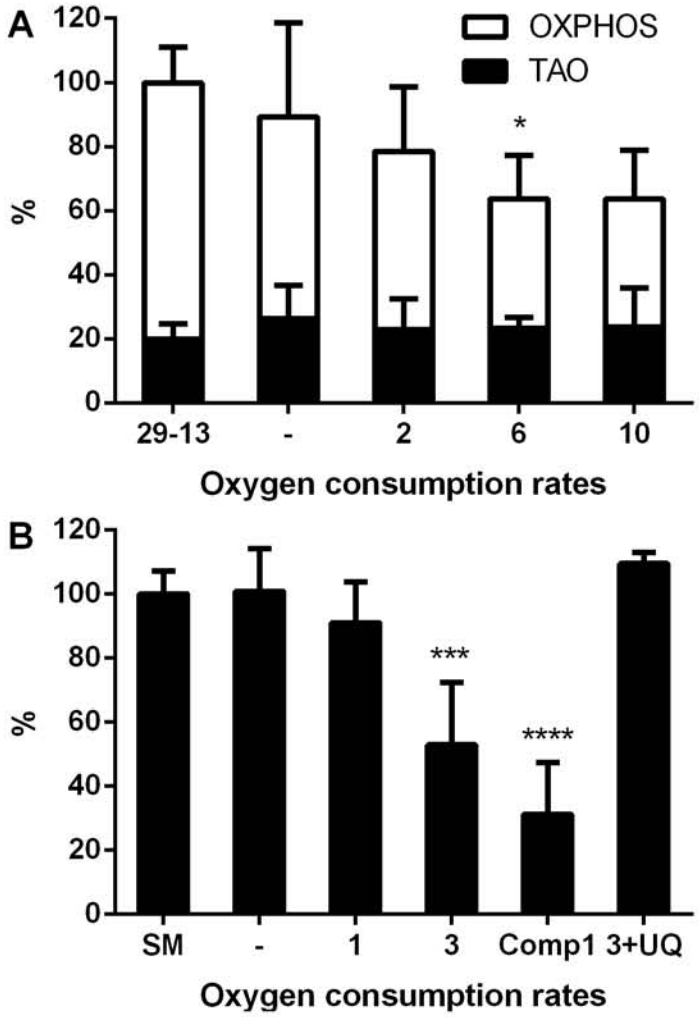

FIG. 3. Effect of TbSPPS RNAi on oxygen consumption rate in the procyclic (A) and bloodstream (B) cells. (A) For procyclics, the relative contribution of alternative pathway via trypanosome alternative oxidase (TAO; black columns) and cytochrome-mediated pathway (white columns) was measured in parental 29-13 cells, non-induced cells (-), and cells 2, 6 and 10 days after RNAi induction. The amount of O2 consumption inhibited by KCN (0.1 mM) reflected the capacity of the cytochrome-mediated pathway, while the amount inhibited by SHAM (0.03 mM) represented the TAO activity. The non-inhibited residual oxygen consumption was considered as zero. The mean and the S.D. values of three experiments are shown. (B) In the absence of the cytochrome-mediated pathway in the bloodstream cells, all respiration is mediated by TAO. Oxygen consumption was measured in parental SM cells, non-induced cells (-), cells after 1 or 3 days RNAi induction, cells after compound 1 (1 μM for 24 hours) inhibition and RNAi cells supplied with UQ10. Statistic significances to control groups were indicated by asterisks (*, $p<0.05$; ***, $p<0.0005$; ****, $p<0.00005$).

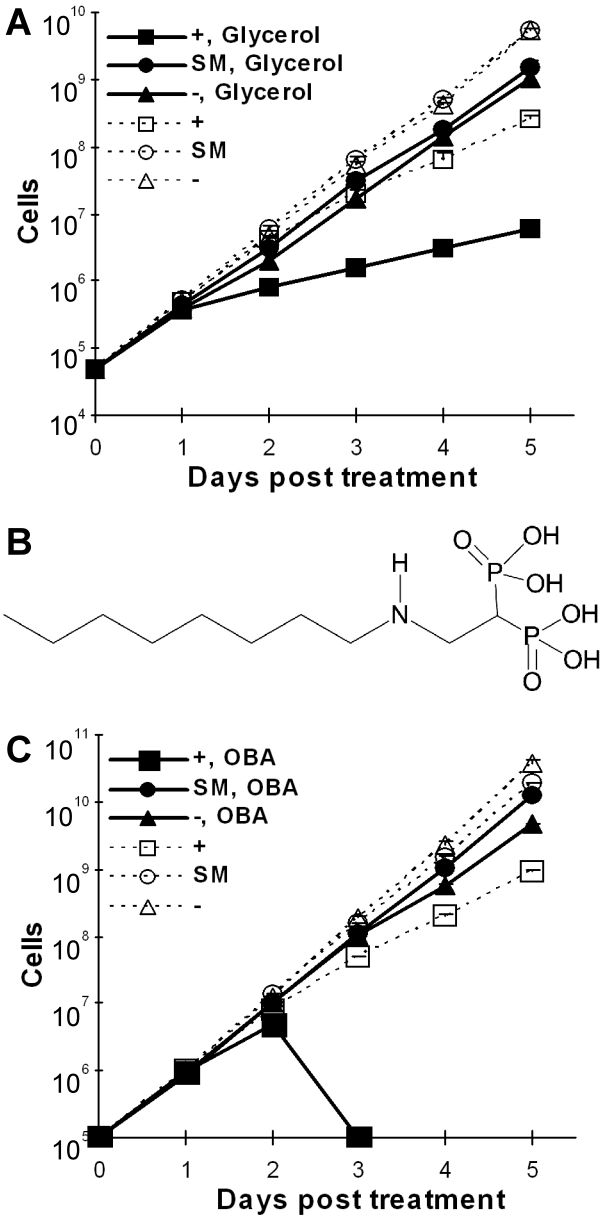

FIG. 4. Growth curve of bloodstream transfectant cells in the presence of glycerol or compound 1. (A) The addition of 4 mM glycerol to the medium had an inhibitory effect on the TbSPPS knock-downs after RNAi induction (continuous line with full squares), while only mild effect was observed for the SM parentals (continuous line with full circles) and non-induced cells (continuous line with full triangles). The same cell lines were grown in the absence of glycerol as controls (dotted lines). (B) Chemical structure of 1-[(n-oct-1-ylamino)ethyl] 1,1-bisphosphonic acid (compound 1), a potent inhibitor of the enzymatic acitivity of TcSPPS. (C) The addition of 1 μM compound 1 to the medium was lethal to the RNAi-induced TbSPPS knock-downs (continuous line with full squares), while just a very small effect was observed for the SM parentals (continuous line with full circles) and the non-induced cells (continuous line with full triangles). The same cell lines were grown in the absence of compound 1 as controls (dotted lines). The experiment was repeated three times, a representative curve is shown.

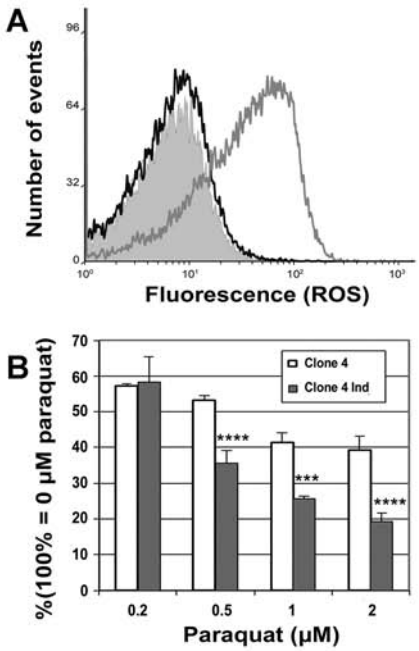

FIG. 5. Reactive oxygen species generation (A) and paraquat treatment (B) in the TbSPPS procyclic cells. (A) Parental 29-13 cells (open area with black line), non-induced cells (gray area) and procyclic cells 6 days after RNAi induction (open area with gray line) were incubated in the presence of 5 mg ml-1 dihydroethidium for 30 min. The fluorescence distributions measured by flow cytometry were plotted as frequency histograms. (B) Growth of non-induced procyclics and cells 5 days after RNAi induction in the presence of 0.2, 0.5, 1 and 2 µM paraquat for 3 additional days. The growth of cells in the absence of paraquat, either non-induced or RNAi-induced, was considered as 100%.

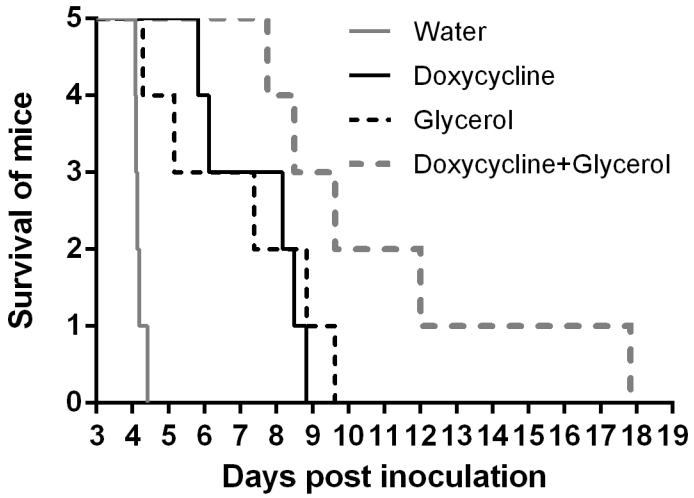

FIG. 6. Survival of mice infected with TbSPPS RNAi transfectant cells was prolonged upon the addition of glycerol and doxycycline. Drinking water available to four groups of mice, each consisting of five individuals, was either pure (gray line), or supplemented with 1 mg ml-1 doxycyline sweetened with 50 mg ml-1 of sucrose (black line), or 5% glycerol (black dotted line), or both doxycycline and glycerol (gray dotted line). The survival of mice was followed on a daily basis.

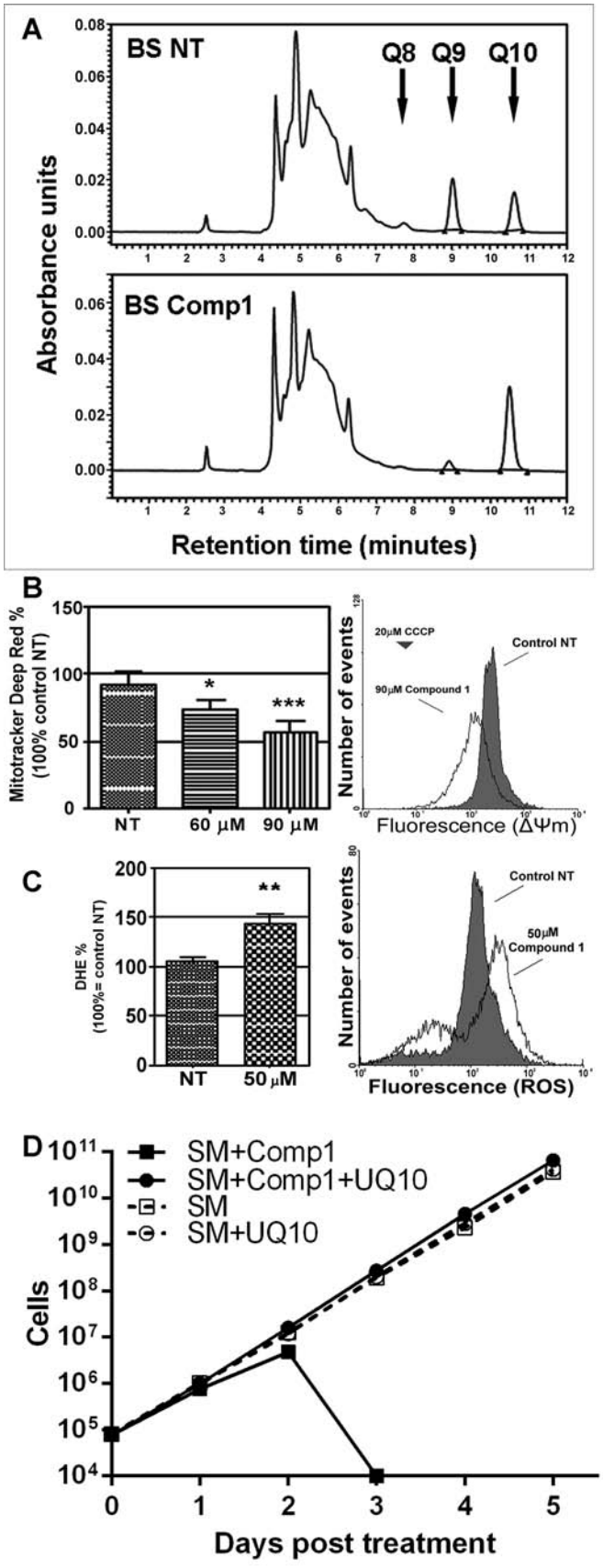

FIG. 7. Metabolic effects of the inhibition by compound 1 on wild type bloodstream parasites. (A) Measurement of the UQ pool. HPLC representative runs for untreated and treated bloodstream stages are shown. The positions of the calibration standards are indicated by arrows. (B) The m displayed by procyclic cells treated with different concentrations of compound 1. Statistical analysis and a representative experiment are presented. Asterisks indicate significant differences in comparison to the control group (untreated parasites). The arrowhead represents the position of the depolarized membrane control CCCP. (C) ROS level in procyclic cells treated for 72 hours with 50 µM compound 1. The data are expressed as means ± standard deviation of at least two independent experiments. (D) Rescue of parental SM bloodstream cells. The addition of 10 µM compound 1 to the medium was lethal within three days (continuous line with full squares). Further addition of 20 µM UQ10 fully rescued cell growth (continuous line with full circles). Non-treated (empty squares) and cells treated only with 20 µM UQ10 (empty circles) were used as controls.